Received: 20 February 2024 | Revised: 9 May 2024 | Accepted: 22 May 2024

DOI: 10.1002/jor.25921

Journal of Orthopaedic Research®

RESEARCH ARTICLE

Aging alters the subchondral bone response 7 days after noninvasive traumatic joint injury in C57BL/6JN mice

Lexia A. Dauenhauer[1] | Brady D. Hislop[2] | Priyanka Brahmachary[2] | Connor Devine[3] | Dustin Gibbs[4] | Ronald K. June[2] | Chelsea M. Heveran[2]

[1]Department of Biomedical Engineering, Montana State University, Bozeman, Montana, USA

[2]Department of Mechanical & Industrial Engineering, Montana State University, Bozeman, Montana, USA

[3]Department of Chemical Engineering, Montana State University, Bozeman, Montana, USA

[4]Gallatin College, Montana State University, Bozeman, Montana, USA

Correspondence
Chelsea M. Heveran, Department of Mechanical & Industrial Engineering, Montana State University, Bozeman, MT, USA.
Email: chelsea.heveran@montana.edu

Funding information
National Institute of General Medical Sciences, Grant/Award Number: P20GM103474; National Institute on Aging, Grant/Award Number: R03AG068680; National Institute of Arthritis and Musculoskeletal and Skin Diseases, Grant/Award Number: R01AR073964; Division of Civil, Mechanical and Manufacturing Innovation, Grant/Award Numbers: 1554708, 2120239

Abstract

Posttraumatic osteoarthritis (PTOA) commonly develops following anterior cruciate ligament (ACL) injuries, affecting around 50% of individuals within 10–20 years. Recent studies have highlighted early changes in subchondral bone structure after ACL injury in adolescent or young adult mice, which could contribute to the development of PTOA. However, ACL injuries do not only occur early in life. Middle-aged and older patients also experience ACL injuries and PTOA, but whether the aged subchondral bone also responds rapidly to injury is unknown. This study utilized a noninvasive, single overload mouse injury model to assess subchondral bone microarchitecture, turnover, and material properties in both young adults (5 months) and early old age (22 months) female C57BL/6JN mice at 7 days after injury. Mice underwent either joint injury (i.e., produces ACL tears) or sham injury procedures on both the loaded and contralateral limbs, allowing evaluation of the impacts of injury versus loading. The subchondral bone response to ACL injury is distinct for young adult and aged mice. While 5-month mice show subchondral bone loss and increased bone resorption postinjury, 22-month mice did not show loss of bone structure and had lower bone resorption. Subchondral bone plate modulus increased with age, but not with injury. Both ages of mice showed several bone measures were altered in the contralateral limb, demonstrating the systemic skeletal response to joint injury. These data motivate further investigation to discern how osteochondral tissues differently respond to injury in aging, such that diagnostics and treatments can be refined for these demographics.

KEYWORDS
ACL injury, aging, posttraumatic osteoarthritis, subchondral bone

1 | INTRODUCTION

An estimated 400,000 people receive anterior cruciate ligament (ACL) reconstructive surgery annually in the United States alone[1] with approximately 50% of people developing posttraumatic osteoarthritis (PTOA) within 10–20 years,[2] regardless of surgery status. While the majority of patients that experience ACL injury are adolescents or younger adults, 11.4% of these patients are over the age of 46.[3] This demographic of middle-aged or older patients experiencing ACL injury is growing as the population ages.[4] Numerous studies demonstrate that in

humans and rodents, subchondral bone plays an important role in the early response to ACL injury, which precedes development of PTOA.[5–10] However, the early response of subchondral bone to ACL injury in the aged knee is undetermined. This gap in knowledge limits the evaluation and treatment of detrimental joint changes following ACL injury in aged populations.

Subchondral bone, composed of cortical bone in the subchondral bone plate and supporting trabecular bone in the epiphysis, is an important contributor to joint changes following ACL injury.[11] Subchondral bone not only supports cartilage by absorbing shock from mechanical stimulus, but also participates in crosstalk with cartilage.[11,12] Subchondral bone is a dynamic structure, and both the subchondral bone plate and epiphysis are observed to thin in early-stage osteoarthritis in both humans and rodents.[9,13–15] However, with time, the subchondral bone plate reverses course to become sclerotic while the epiphysis does not recover from its initial bone loss.[9,12,16,17] The rapid changes to subchondral bone soon after joint injury are the product of altered bone turnover[14] and potentially precede changes to cartilage.[12,18] In young adult mice, these early changes to subchondral bone plate structure, evident at 7 days after injury, occur concurrently with elevated osteoclast abundance and altered synovial fluid metabolism.[10] However, whether subchondral bone rapidly responds to injury in the aged knee is unknown.

The subchondral bone response to ACL injury may well differ with age, since aging introduces many structural and biological differences to the knee joint.[19–23] Aged joints have decreased mesenchymal stem cells,[21] increased inflammation,[20] and a decreased immune response.[19] In mice, mineralization of the epiphysis decreases with aging,[24] although changes in microarchitecture can be more mild than observed in the metaphysis.[25] The aged joint is also more likely to have baseline cartilage damage before ACL injury from various things including other injuries or "wear-and-tear" osteoarthritis.[11,12,14] However, very few studies have investigated the response of aged knees to injury, especially at early timepoints postinjury (Table 1). It remains to be tested whether the subchondral bone plate thickness, epiphyseal microarchitecture, and subchondral bone plate material properties of aged mice show a similar early response to injury as younger mice.

The objective of this study was to test whether the early subchondral bone response to joint injury differs between young adult (5 months, ~20-year-old human) and early old age (22 months, ~60-year-old human) C57BL/6JN mice.[26] This study utilized a noninvasive, single-overload mouse injury model that simulates human ACL injuries without the confounding effects of surgery.[7,9,10,17,27–29] Subchondral bone plate and epiphyseal microarchitecture, tissue-scale modulus, osteoclast abundance, and bone formation were evaluated 7 days after injury for injured and sham-injured limbs and their contralateral controls.

2 | MATERIALS AND METHODS

2.1 | Mouse model of ACL injury

All animal procedures were approved by Montana State University IACUC. All mice were group housed (≤5 mice per cage). Female C57BL/6JN mice were randomly assigned to either injured (n = 8 young, n = 11 old) or sham-injured (n = 8 young, n = 10 old) groups and a limb was randomly assigned (i.e., left or right) as the loaded limb. Both groups received a preload of 1–2 N on the loading limb from a custom apparatus.[10] Mice in the injured group then received an additional 12–15 N load (Figure 1). Joint injuries were confirmed by the characteristic release in load as well as a pre- and postinjury joint laxity tests to assess anterior stability, which are both indicators of an ACL tear.[9,37,38] Due to synovial fluid extraction at euthanasia, we were not able to directly confirm ACL tears. Mice were initially anesthetized (2%–4% isoflurane, 30 s) in an inhalation chamber. During loading, a nose cone (2% isoflurane) was used to maintain anesthesia. Mice were monitored every day until euthanasia at 7 days after injury by cervical dislocation and the hind limbs were dissected. Data from the 5-month mice were published in an earlier paper from our group.[10] This study re-analyzes these data together with new data from 22-month mice.

2.2 | MicroCT analysis of epiphyseal and subchondral plate microarchitecture

Tibiae were separated from femurs, cleaned of non-osseous tissue, placed in 70% ethanol, and refrigerated at 4°C. The proximal tibiae were evaluated for microarchitecture of the subchondral bone plate and epiphysis (μCT40, Scanco Medical AG, 10 μm isotopic voxel size, 70 kVP, 114 μA, 200 ms integration time). The epiphysis was evaluated for bone volume fraction (BV/TV, %), bone mineral density (BMD, mgHA/cm^3), trabecular number (Tb.N, 1/mm), trabecular spacing (Tb.Sp, mm), and trabecular thickness (Tb.Th, mm). The subchondral bone plate was evaluated for bone plate thickness and tissue mineral density (TMD, mgHA/cm^3) for both the medial and lateral aspects.

2.3 | Nanoindentation analysis of subchondral bone plate tissue-scale modulus

After microCT analyses, tibiae were dehydrated in a graded ethanol series, cleared with acetone, embedded in poly(methyl)methacrylate (PMMA), sectioned with a low-speed saw, and polished with 9–0.5 μm alumina suspensions to achieve a mirror finish. Polished samples were indented (KLA-Tencor iMicro) on the coronal plane between the tidemark and epiphysis spanning from the medial to lateral aspects of the subchondral bone plate (N = 8-12 indents per sample, Figure 2). A Berkovich tip and a trapezoidal load profile of 5 mN (30 s to load, 60 s hold, 30 s unload) were used. The modulus was calculated from the contact stiffness and tip area function, per the Oliver-Pharr method.[39] The contact stiffness was taken from the derivative at an initial point of a polynomial fit to the 95th–20th percentiles of the unloading curve. The tip area function was calibrated on silica.

TABLE 1 Literature review of early subchondral bone response to joint injuries in mice.

Reference	Rodent model	Mouse age(s)	Injury model	Evaluation time point(s)	Region(s) of interest	Acute bone response to injury
[9]	Male C57BL/6N	10 weeks	Noninvasive anterior cruciate ligament (ACL) rupture	1, 3, 7, 14, 28, 56 days	Epiphysis, subchondral bone	*Epiphysis* ↓ Bone volume fraction (BV/TV), bone mineral density (BMD), Tb.Th at 7 days after injury *Subchondral bone plate* ↓ Thickness at 7 days after injury
[30]	Male FVB mice	3 months	ACL rupture and 240-cycle compression	1 and 8 weeks	No bone measures evaluated	Not evaluated
[7]	Female C57BL/6 mice	12 weeks	Noninvasive ACL rupture	7, 14, 21, 28 days	Epiphysis	*Epiphysis* ↓ BV/TV and trabecular thickness (Tb.Th) at 7 days after injury
[6]	Male wild-type C57BL/6 mice	10 weeks	DMM, articular cartilage scratches (CS), combination (DCS)	7, 14, 28 days	Epiphysis, subchondral bone	*Epiphysis* No trabecular bone differences 7 days after injury *Subchondral bone* ↑ Osteophyte formation 7 days after DCS ↑ Osteosclerosis 7 days after all injuries
[31]	Female and male C57BL/6 mice	20 weeks	Noninvasive ACL rupture	7 days	Epiphysis	*Epiphysis* ↓ BV/TV and Tb.Th at 7 days after injury
[27]	Female C57BL/6N mice	10 weeks	Noninvasive ACL rupture	7 and 14 days	Epiphysis	*Epiphysis* ↓ BV/TV and Tb.Th at 7 days after injury
[32]	Male C57BL/6 mice	10 and 26 weeks	Cyclic compression	1, 2, and 6 weeks	Epiphysis, subchondral bone	*Epiphysis* ↓ BV/TV and Tb.Th with 9N of load *Subchondral bone* ↑ Thickness in 10-week mice w/9N ↓ Thickness in 26-week mice w/9N
[33]	Female C57Bl6 mice	8 weeks	DMM, ACLT, and ACLR	2 weeks	Subchondral bone	*Subchondral bone* ↓ Thickness 14 days after injury ↓ Modulus 14 days after injury ↓ Mineralization 14 days after injury
[34]	Male Sprache-Dawley rat	10 weeks	ACL transaction model	1, 2, 4, 6, and 10 weeks	Epiphysis	*Epiphysis* ↓ BV/TV 14 days after injury ↑ Osteophyte formation 7 days after injury
[35]	Female Sprague Dawley rats	14–16 weeks	Noninvasive ACL rupture	2, 4, 8 weeks	Epiphysis	*Epiphysis* ↑ Calcein label 14 days after injury ↓ BV/TV 14 days after injury
[36]	Female Lewis rat	14 weeks	Noninvasive ACL rupture	3, 7, 10, and 14 days	Epiphysis, Subchondral bone	*Epiphysis* ↓ BV/TV, tissue mineral density (TMD), and BMD with injury *Subchondral bone* ↓ Thickness, BV/TV, TMD with injury

2.4 | Histological analysis of osteoclast number density

Femurs were placed in 10% neutral buffered formalin (NBF) for 18 h, decalcified in EDTA, dehydrated in ethanol, embedded in paraffin, and microtomed to 5-μm sagittal sections. Sections were stained with tartrate-resistant acid phosphatase (TRAP) to indicate active osteoclasts in accordance with the manufacturer's directions (Sigma). Stained sections were imaged at the epiphysis using a Nikon Eclipse E-800 brightfield microscope at 4X and 10X. Using ImageJ, the bone surfaces that enclose the marrow cavities from the articular surface to the epiphyseal line were traced in 4X images. Multinucleated

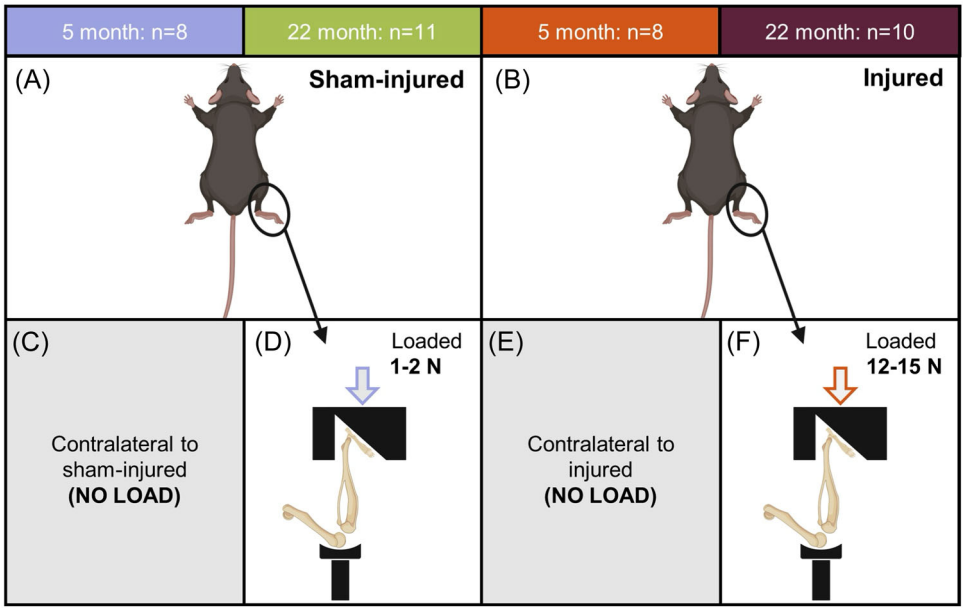

FIGURE 1 Study design to investigate the effects of joint injury versus joint loading on subchondral bone for young adult and aged mice. Mice were randomized into (A) sham-injured or (B) injured groups. (D, F) One randomized limb in each mouse was loaded with 1–2 N (sham-injured) or 12–15 N (joint injury which likely produces anterior cruciate ligament [ACL] tear). (C, E) For all mice, the contralateral limb received no load. Figure made using BioRender.

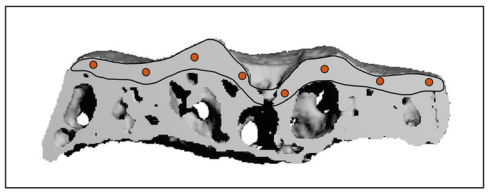

FIGURE 2 Representative nanoindentation locations (red dots) on subchondral bone plate for a 5-month mouse.

TRAP-positive cells were counted from the 10X images. These data were used to calculate the osteoclast number density per area (Oc.N/A) and the osteoclast density per bone surface (Oc.N/BS). Analyses were conducted by 1 evaluator blinded to mouse age, injury, and loading status. Representative TRAP staining images are included in Supporting Information S1: Figure S1.

2.5 | Dynamic histomorphometry analysis of epiphysis bone formation

Calcein (20 mg/kg) and alizarin (30 mg/kg) were injected 3 days before injury and 1 day before euthanasia, respectively, to all study mice. Fluorochrome labels were imaged using a confocal laser scanning microscope (CLSM, inverted Leica SP5 and SP8) on the same embedded and polished tibial specimens used for nanoindentation analyses. Excitation and emission parameters were 488 and 500–550 nm for calcein and 461 and 650–750 nm for alizarin. Z-stacks were collected for medial and lateral epiphyseal regions for each specimen. The voxel size was 1.52 µm by 1.52 µm by 4.74 µm. One in-focus image from each z-stack was selected for analysis. The bone perimeter and calcein and alizarin labels of the epiphyseal region of interest were traced by two evaluators using iPads blinded to mouse identity. The traced images were then analyzed using custom MATLAB code to calculate alizarin/bone surface and calcein/bone surface. Representative dynamic histomorphometry images are included in Supporting Information S1: Figure S2.

2.6 | Statistical analysis

A mixed model analysis of variance (ANOVA) was used to investigate the fixed effects of injury (i.e., injured vs. sham-injured), load (i.e., loaded limb vs. contralateral limb), and their interaction on subchondral bone microarchitecture, osteoclast activity, and bone formation. Mouse identity was a random effect in these models. Separate models were analyzed for 5-month and 22-month mice, since age effects are already well-understood for these measures. However, since the effect of age on subchondral bone modulus has not been investigated, a three-way mixed model ANOVA was employed, with fixed effects of age, injury, and load and a random effect of mouse identity. To test for weight changes associated with joint injury, a three-way mixed model ANOVA included fixed effects of age, injury, and time-point (i.e., before injury at euthanasia) and a random effect of mouse identity. To test for differences in responses between left and right limbs, a two-way mixed model ANOVA included fixed effects of side, injury, and loading and a random effect of mouse identity. For all models, residuals were checked to ensure

they met normality and equal variance. The dependent variable was natural log transformed, if necessary, to satisfy these assumptions. Significance was defined a priori as $p < 0.05$. Significant interactions were followed by Fisher post hoc tests to control family-wise Type I error. Minitab (version 20.3) was used for all analyses.

3 | RESULTS

3.1 | Mouse injuries

Injuries were confirmed from characteristic release in the loading curve, which is expected to produce ACL tears as confirmed in other studies in our lab and others using these loading parameters.[9,10,31] Eight mice in the study sustained tibia plateau injuries as confirmed from microCT and were excluded from all analyses (10% of 5-month mice [$n = 2$], and 28% of 22-month mice [$n = 6$]), Mouse weights were compared at the time of the calcein label injection (3 days before injury) and at euthanasia. There was a significant interaction between time point and injury ($p = 0.021$) such that uninjured mice gained weight after sham-loading procedures, but injured mice did not gain weight. However, this interaction was found to be not significant after post hoc testing.

3.2 | Epiphyseal and subchondral bone microarchitecture

Young adult (5-month) mice showed significant effects of joint injury (i.e., injury vs. sham-injury) and loading (i.e., the injured and sham-injured limbs vs. the contralateral limbs) on microarchitecture of both the epiphysis and the subchondral bone plate (Figure 3). In the epiphysis, BV/TV, BMD, and Tb.Th all decreased with injury (−11.46%, $p = 0.002$; −7.37%, $p = 0.012$; −5.64%, $p = 0.028$, respectively) and loading (−7.89%, $p = 0.023$; −5.92%, $p = 0.040$; −6.17%, $p = 0.017$, respectively). Neither Tb.N nor Tb.Sp were significantly affected by injury, loading, or the interaction of these factors (Table 2). For young mice, subchondral bone plate thickness responded differently to injury and loading for the medial and lateral aspects. The thickness of the lateral subchondral bone plate depended on the interaction of injury and loading ($p = 0.001$). Post hoc testing revealed that the subchondral bone thickness decreased with loading ($p < 0.001$, 16.81%) for the injured but not sham-injured mice. For the medial aspect, subchondral bone plate thickness did not depend on injury, loading, nor the interaction of these factors. For both lateral and medial sides, subchondral bone plate TMD showed an interactive effect of injury and loading ($p < 0.001$, $p = 0.040$, respectively). Post hoc testing determined that for the lateral side, subchondral bone plate TMD decreased with loading for the injured mice ($p < 0.001$, 4.54%) but not sham-injured mice (Table 2). After post hoc testing, there were no significant effects of TMD on the medial aspect. There were no significant effects of injury, loading, nor their interaction on measures of epiphyseal microarchitecture for 22-month mice. In addition, there were no effects of injury or loading on measures of subchondral bone thickness or TMD, medially or laterally (Figure 3) (Table 3).

3.3 | Epiphyseal osteoclast abundance

For 5-month mice, the osteoclast number per bone surface (Oc.N/BS) and osteoclast number per area (Oc.N/A) both increased with injury

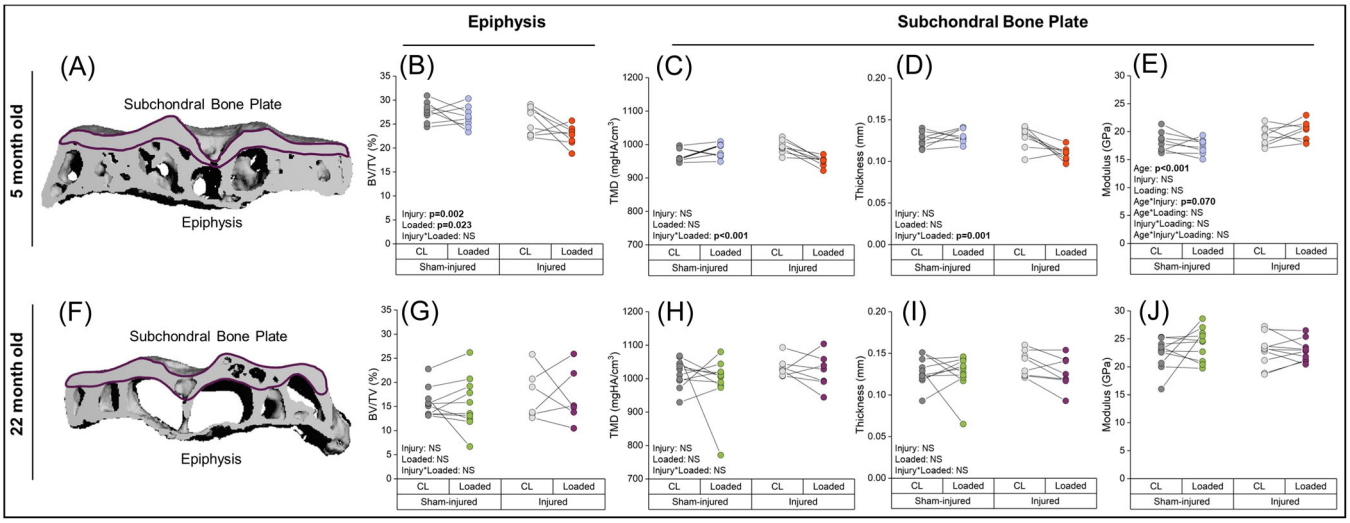

FIGURE 3 The effects of aging, injury, and loading on epiphyseal and subchondral bone microarchitecture, mineral density, and modulus. (A, F) MicroCT images show the dramatic changes in microarchitecture with aging. Outlined regions represent the subchondral bone plate ROI. (B–E) For 5-month-old mice, injury and loading decrease epiphyseal BV/TV, subchondral bone plate thickness, and tissue mineral density (TMD). (G–J) For 22-month-old mice, there are no significant effects of injury or loading on epiphyseal nor subchondral bone plate microarchitecture. (E, J) A two-way mixed model analysis of variance (ANOVA) tested the dependence of subchondral bone plate modulus on age, injury, and loading. The results of this ANOVA are shown in (E), but repeated measures plots are separated by age (E–J) for clarity.

(95.49%, $p = 0.016$; 90.79%, $p = 0.017$, respectively). There were no significant effects of loading nor an interaction between injury and loading on either measure (Figure 4) (Table 4). For 22-month mice, the osteoclast number per bone surface (Oc.N/BS) and osteoclast number per area (Oc.N/A) both decreased with injury (−77.88%, $p = 0.015$; −31.86% $p = 0.022$, respectively). Consistent with the younger mice, there were no significant effects of loading nor an interaction between injury and loading on measures of osteoclast abundance (Figure 4; Table 5).

3.4 | Epiphyseal bone formation

Calcein labels were injected 3 days before injury and alizarin labels were injected 6 days after injury (1 day before euthanasia). For 5-month mice, there was a significant decrease in calcein-to-bone surface with loading (20.13%, $p = 0.005$). In other words, compared with the contralateral limb, loaded limbs (both the injured and sham-injured groups) had less calcein label retention. There were no significant effects of injury or the interaction of the two factors (Figure 4) (Table 4). While not statistically significant, the 22-month mice show a trend of decreased calcein-to-bone surface with loading (12.86%, $p = 0.072$). Injury did not significantly impact calcein-to-bone surface for these older mice (Figure 4) (Table 5). For both 5-month and 22-month mice, there were no significant effects of injury, loading, nor an interaction of these factors on alizarin-to-bone surface.

3.5 | Subchondral bone plate modulus

The modulus of the subchondral bone plate, evaluated using nanoindentation, substantially increased from 5 to 22 months (21.74%, $p < 0.001$). There was a trend of an interaction between injury and age ($p = 0.070$) where there was no change in modulus with injury in the 22-month-old mice (−1.39%), but an increase of modulus with injury in the 5-month-old mice (9.58%). The subchondral bone plate modulus did not depend on the loaded side, or interactions between loading and the factors of injury or age (Figure 3) (Table 6).

3.6 | Effect of left/right side on subchondral bone measures in response to injury

Since mice have been shown to have important differences in trabecular morphometry from left to right sides,[40] we randomized which limb was subjected to injuries or sham-injuries. We also ran three-factor ANOVAs that included the factor of the side that was loaded (i.e., left or right) in addition to the factors of injury (i.e., 12–15 N load vs. 1–2 N load) and

TABLE 2 Epiphyseal and subchondral bone plate microarchitecture for 5-month-old mice.

	Control		Injured			
	Contralateral-to-sham $n = 8$	Sham-injured $n = 8$	Contralateral-to-injured $n = 8$	Injured $n = 8$	Main effects	Two-way interactions
Proximal tibia epiphysis						
Bone volume fraction (BV/TV) (%)	27.57 ± 2.16	26.51 ± 2.28	25.60 ± 2.91	22.63 ± 2.09	Injury: $p = 0.002$ Loaded: $p = 0.023$	NS
Bone mineral density (mgHA/cm^3)	345.50 ± 21.26	337.25 ± 24.76	332.50 ± 29.57	301.75 ± 26.31	Injury: $p = 0.012$ Loaded: $p = 0.040$	NS
Trabecular number (1/mm)	4.05 ± 0.28	3.97 ± 0.33	3.99 ± 0.26	3.97 ± 0.13	NS	NS
Trabecular thickness (mm)	0.07 ± 3.9e-3	0.07 ± 5.1e-3	0.07 ± 4.6e-3	0.07 ± 5.5e-3	Injury: $p = 0.028$ Loaded: $p = 0.017$	NS
Trabecular spacing (mm)	0.26 ± 0.02	0.26 ± 0.03	0.26 ± 0.02	0.26 ± 0.01	NS	NS
Subchondral bone plate						
Medial thickness (mm)	0.15 ± 0.01	0.15 ± 0.01	0.14 ± 0.01	0.13 ± 0.02	NS	NS
Medial tissue mineral density (TMD) (mgHA/cm^3)	981.60 ± 33.50	992.50 ± 17.29	991.4 ± 31.20	954.3 ± 39.80	NA	Injury × Loaded: $p = 0.040$
Lateral thickness (mm)	0.13 ± 9.4e-3	0.13 ± 8.5e-3	0.13 ± 0.01	0.11 ± 0.01	NA	Injury × Loaded: $p = 0.001$
Lateral TMD (mgHA/cm^3)	968.38 ± 19.81	982.13 ± 21.13	993.75 ± 19.62	949.63 ± 14.38	NA	Injury × Loaded: $p < 0.001$

TABLE 3 Epiphyseal and subchondral bone plate microarchitecture for 22-month-old mice.

	Control		Injured			
	Contralateral-to-sham $n = 10$	Sham-Injured $n = 10$	Contralateral-to-injured $n = 7$	Injured $n = 7$	Main effects	Two-way interactions
Proximal tibia epiphysis						
Bone volume fraction (BV/TV) (%)	15.82 ± 3.06	15.74 ± 5.48	17.57 ± 5.19	17.00 ± 5.72	NS	NS
Bone mineral density (mgHA/cm^3)	251.90 ± 28.78	246.80 ± 67.00	256.70 ± 51.20	255.50 ± 60.80	NS	NS
Trabecular number (1/mm)	2.55 ± 0.37	2.86 ± 0.78	2.84 ± 0.32	3.11 ± 0.80	NS	NS
Trabecular thickness (mm)	0.08 ± 6.3e-3	0.07 ± 7.1e-3	0.07 ± 9.9e-3	0.07 ± 6.4e-3	NS	NS
Trabecular spacing (mm)	0.45 ± 0.06	0.41 ± 0.09	0.40 ± 0.05	0.37 ± 0.10	NS	NS
Subchondral bone plate						
Medial thickness (mm)	0.16 ± 0.02	0.15 ± 0.02	0.16 ± 0.02	0.15 ± 0.03	NS	NS
Medial tissue mineral density (TMD) (mgHA/cm^3)	1033.40 ± 28.10	1025.50 ± 86.90	1044.70 ± 31.50	1034.60 ± 52.40	NS	NS
Lateral thickness (mm)	0.13 ± 0.02	0.13 ± 0.02	0.14 ± 0.02	0.13 ± 0.02	NS	NS
Lateral TMD (mgHA/cm^3)	1014.80 ± 43.20	988.80 ± 82.70	1033.30 ± 29.20	1022.40 ± 52.00	NS	NS

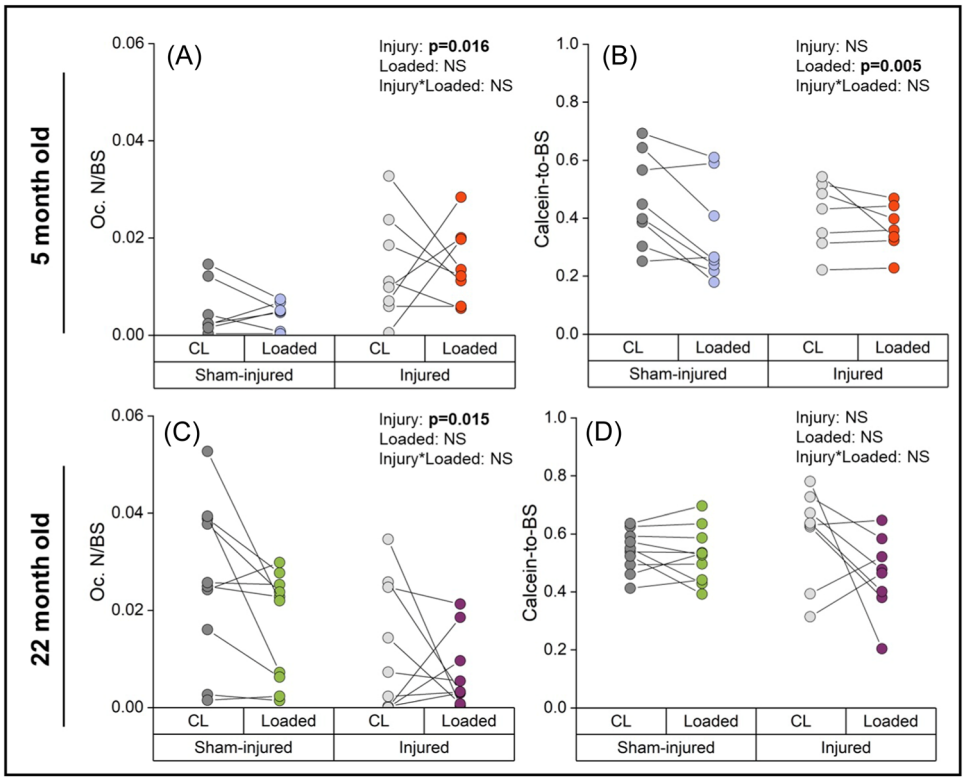

FIGURE 4 The effects of injury and loading on bone formation and osteoclast activity. (A, B) For 5-month mice, injury increases osteoclast abundance. Loading decreased calcein-labeled epiphyseal surfaces, indicating resorption since this fluorochrome label was delivered before the joint injuries. (C, D). For 22-month mice, osteoclast abundance decreased with injury but no changes were found for calcein labels.

loaded side (i.e., whether the limb received the load vs the contralateral side). From these additional ANOVA models, we learned that side significantly impacted two measures, Oc.N/BS and Oc.N/A, for young but not old mice. For these measures, the left side had 72% ($p = 0.025$) and 75% ($p = 0.047$) more osteoclasts than the right side. Importantly, even when the factor of side was included in the model, these measures of osteoclast number density were still increased with injury (+95.49%, $p = 0.016$; +90.79%, $p = 0.017$, respectively).

TABLE 4 Subchondral bone turnover for 5-month-old mice.

	Control		Injured			
	Contralateral-to-sham $n = 8$	Sham-Injured $n = 8$	Contralateral-to-injured $n = 8$	Injured $n = 8$	Main effects	Two-way interactions
Oc.N/BS (%)	5.32e-3 ± 5.64e-3	4.26e-3 ± 2.75e-3	1.37e-2 ± 1.06e-2	1.46e-2 ± 7.77e-3	Injury: $p = 0.016$	NS
Oc.N/A (%)	2.08e-4 ± 2.62e-4	1.84e-4 ± 1.27e-4	5.53e-4 ± 4.27e-4	5.28e-4 ± 3.05e-4	Injury: $p = 0.017$	NS
Calcein-to-BS	46.10 ± 15.88	34.54 ± 17.03	40.85 ± 11.81	36.50 ± 8.09	Loaded: $p = 0.005$	NS
Alizarin-to-BS	42.28 ± 15.47	33.44 ± 19.97	37.63 ± 12.04	46.30 ± 23.76	NS	NS

TABLE 5 Subchondral bone turnover for 22-month-old mice.

	Control		Injured			
	Contralateral-to-sham $n = 10$	Sham-Injured $n = 10$	Contralateral-to-injured $n = 10$	Injured $n = 10$	Main effects	Two-way interactions
Oc.N/BS (%)	2.64e-2 ± 1.65e-2	1.94e-2 ± 1.36e-2	1.22e-2 ± 1.33e-2	7.27e-3 ± 7.70e-3	Injury: $p = 0.015$	NS
Oc.N/A (%)	6.21e-4 ± 3.55e-4	5.27e-4 ± 3.35e-4	5.96e-4 ± 8.26e-4	2.31e-4 ± 2.55e-4	Injury: $p = 0.022$	NS
Calcein-to-BS	54.06 ± 7.10	52.73 ± 9.43	59.76 ± 16.09	46.01 ± 13.61	Loaded: $p = 0.072$	NS
Alizarin-to-BS	18.01 ± 6.71	23.15 ± 10.23	24.55 ± 14.89	32.10 ± 16.35	NS	NS

4 | DISCUSSION

Recently, the subchondral bone response to ACL injury has gained attention as one of the first detectable changes in the trajectory of joint degeneration after an injury.[11,12] In previous work by us and others, young mice (10 weeks–5 months) demonstrate early subchondral and epiphyseal bone loss, increased osteoclast abundance, and altered joint metabolism soon (7–14 days) after ACL injury.[9,10,17,27,38] These data help to establish subchondral bone as a potentially important treatment target for mitigating PTOA. Despite the fact that ACL injuries are not uncommon among middle-aged and older adults,[3] little attention has been given to the response of aging joints to such injuries. The purpose of the present investigation was to determine whether early-old aged mice (22 months) would also display an acute subchondral bone response to joint injury compared with young adult (5 months) mice.

Aging is well-known to decrease bone architecture in female C57BL/6JN mice. When comparing sham-injured limbs, older mice had 54.2% reduced BV/TV and 39.87% reduced Tb.N of the epiphysis (Figure 3), consistent with our expectation of decreased cancellous microarchitecture with aging.[41] The subchondral bone plate was thicker for aged mice and, reported for the first time in this study, more than 20% stiffer than for young mice. Older mice also had increased osteoclast activity, with Oc./BS and Oc.N/A in the sham-injured mice increasing with age by 115.62% and 89.10%, respectively. These data demonstrate that the aged knee has an altered structural and biological environment, even in the absence of a joint injury.

Our data show that young and old mice do not show the same early response to knee injury. The 5-month mice exhibited decreases in epiphyseal microarchitecture and subchondral bone plate thickness and increases in osteoclast abundance with injury, as reported in our previous publication.[10] Loading was seen to change bone turnover. Compared with the contralateral limb, the loaded limb had decreased calcein labeling. Since calcein labels were delivered 3 days before injuries, this result could signify that either loading interrupted label formation or increased bone resorption. Aged mice (22 months) show a different response to joint injury. These mice do not experience loss of epiphyseal or subchondral bone 7 days after injury. Osteoclast activity, already elevated in aging, was decreased with injury. The subchondral bone modulus shows a trend towards increasing with injury for young, but not aged mice. However, our study was likely underpowered to detect this difference. The stiffness of subchondral bone is important for bone mechanotransduction and potentially for fluid transport between the two tissues. It is worth noting that, while not statistically significant, the BV/TV in aged mice increased by 9.25%, which aligns with the decrease in osteoclast density.

The aging knees in this study are likely have a degree of osteoarthritis before injury, which is common in aged mice and humans even in the absence of a joint injury.[11,12,16,22,41] There are other important changes in the aging knee that could alter the response to joint injury. For instance, aging increases inflammation,[20] which could blunt the responsiveness of the joint to injury. It is not known whether the subchondral bone response to injury is slower in aged mice, but this is a possibility. In other contexts, such as hindlimb unloading, discernible bone loss takes longer for aged (18 months)

TABLE 6 Subchondral bone tissue-scale nanoindentation modulus.

	5-month-old				22-month-old						
	Control		Injured		Control		Injured				
	Contralateral-to-sham $n = 8$	Sham-Injured $n = 8$	Contralateral-to-injured $n = 8$	Injured $n = 8$	Contralateral-to-sham $n = 8$	Sham-injured $n = 8$	Contralateral-to-injured $n = 8$	Injured $n = 8$	Main effects	Two-way interactions	3-way interactions
Modulus (GPa)	18.25 ± 1.77	17.35 ± 1.38	19.24 ± 1.70	20.10 ± 1.79	23.42 ± 2.10	24.02 ± 2.97	22.90 ± 2.82	22.88 ± 1.92	Age: $p < 0.001$	Age × Injury: $p = 0.070$	NA

versus young adult (3 months) mice.[42] In future work, additional time points would be valuable to discern the progression of subchondral bone response after joint injury in older mice. Osteocytes, which are important for managing osteoblast bone formation and osteoclast bone resorption, decline in viability in aging and may be less responsive to injury. However, that hypothesis is not specifically tested here. Further, while the early response to injury clearly differs with age, whether the timeline of the aged response to injury is the same in aged mice is not known and would benefit from additional investigation.

Importantly, our study found systemic effects of joint injury on bone outcomes at both ages. In 5 month mice, the contralateral nonloaded limb, experienced epiphyseal and subchondral bone loss similar to the injured limb. In both young and aged mice, there were also systemic effects of injury on measures of osteoclast abundance. These data demonstrate that joint injury does not have isolated skeletal effects at any age and underscores the importance of including non-injured controls in these types of investigations.

The study had several limitations. Our noninvasive loading protocol is expected to have produced ACL injury, given the characteristic response seen for the load versus displacement curves during the joint loading.[9,10,31] However, we were not able to visually confirm ACL tears at dissection because this was precluded by synovial fluid collection from the joint. We excluded mice from the study if there was microCT evidence of tibia plateau fracture to reduce the variability in traumatic joint injury. Only females were included given our availability of aged mice. However, there are important sex differences in bone physiology and the response to joint injury.[12,22] In addition, this study was focused on an early time point (7 days) after injury. Including multiple timepoints would enable evaluation of the progression of joint changes following ACL injury and would be valuable. Likewise, extending the study to measure cartilage outcomes would be useful. Several measures (e.g., subchondral bone plate modulus) may be underpowered and would benefit from the enrollment of additional mice.

In summary, this study demonstrates that the early subchondral bone response to joint injury is not the same for young adult and early old-age female C57BL/6 JN mice. The rapid structural and biological changes observed in the young joint are not recapitulated in aging, which indicates that either the response to injury, or the timeline of this response, is sensitive to aging. Since subchondral bone has important impacts to the physiology and mechanics of the rest of the joint, these data demonstrate that the aging knee joint should not be assumed to respond similarly to younger knees to ACL injury. These age-dependent subchondral bone responses to joint injury highlight the need for including an expanded range of ages in studies of the joint changes that precede and participate in the development of PTOA.

AUTHOR CONTRIBUTIONS

Lexia A. Dauenhauer: Formal analysis; investigation; data curation; writing—original draft; writing—review and editing; visualization. **Brady D. Hislop:** Conceptualization; methodology; software; investigation;

writing—review and editing; supervision. **Priyanka Brahmachary:** Investigation; writing—review and Editing. **Connor Devine:** Investigation; writing—review and Editing. **Dustin Gibbs:** Investigation; writing—review and editing. **Ronald K. June:** Resources; writing—review and editing; funding acquisition. **Chelsea M. Heveran:** Conceptualization; resources; writing—original draft; writing—review and editing; supervision; project administration; funding acquisition.

ACKNOWLEDGMENTS

This work represents the views of the authors and not necessarily those of the sponsors. We appreciate assistance with microCT analyses from the Center for Advanced Orthopedic Studies μCT Core at Beth Israel Deaconness Medical Center as well as assistance with histological sample preparation from Maria Jerome (Montana State University). Hope Welhaven and Ebru Erdogan are thanked for their assistance with mouse dissections. Susanne Dauenhauer is gratefully acknowledged for her help in reviewing and editing during the writing process. This research was made possible by the Department of Mechanical & Industrial Engineering, the College of Engineering, and the Undergraduate Scholars Program at the Montana State University. This work was supported by the National Institutes of Health (NIAMS R01AR073964 [Ronald K. June], NIGMS P20GM103474 [Lexia A. Dauenhauer], NIA R03AG068680 [Chelsea M. Heveran]), and the National Science Foundation (2120239 [Chelsea M. Heveran], 1554708 [Ronald K. June]).

ORCID

Lexia A. Dauenhauer https://orcid.org/0009-0002-5665-1606
Connor Devine http://orcid.org/0000-0003-3986-8141

REFERENCES

1. Vavken, P, Murray, MM. ACL injury epidemiology. In: Murray MM, Vavken P, Fleming BC, eds. *The ACL Handbook*. Springer New York; 2013:3-17.
2. Lohmander LS, Englund PM, Dahl LL, Roos EM. The long-term consequence of anterior cruciate ligament and meniscus injuries. *Am J Sports Med*. 2007;35(10):1756-1769.
3. Schilaty ND, Nagelli C, Bates NA, et al. Incidence of second anterior cruciate ligament tears and identification of associated risk factors from 2001 to 2010 using a geographic database. *Orthop J Sports Med*. 2017;5(8):232596711772419.
4. Mall NA, Chalmers PN, Moric M, et al. Incidence and trends of anterior cruciate ligament reconstruction in the United States. *Am J Sports Med*. 2014;42(10):2363-2370.
5. Pauly HM, Larson BE, Coatney GA, et al. Assessment of cortical and trabecular bone changes in two models of post-traumatic osteoarthritis. *J Orthop Res*. 2015;33(12):1835-1845.
6. McCulloch K, Huesa C, Dunning L, et al. Accelerated posttraumatic osteoarthritis in a dual injury murine model. *Osteoarthr Cartil*. 2019;27(12):1800-1810.
7. Hsia AW, Jbeily EH, Mendez ME, et al. Post-traumatic osteoarthritis progression is diminished by early mechanical unloading and anti-inflammatory treatment in mice. *Osteoarthr Cartil*. 2021;29(12):1709-1719.
8. Coughlin TR, Kennedy OD. The role of subchondral bone damage in post-traumatic osteoarthritis. *Ann NY Acad Sci*. 2016;1383(1):58-66.
9. Christiansen BA, Anderson MJ, Lee CA, Williams JC, Yik JHN, Haudenschild DR. Musculoskeletal changes following non-invasive knee injury using a novel mouse model of post-traumatic osteoarthritis. *Osteoarthr Cartil*. 2012;20(7):773-782.
10. Hislop BD, Devine C, June RK, Heveran CM. Subchondral bone structure and synovial fluid metabolism are altered in injured and contralateral limbs 7 days after non-invasive joint injury in skeletally-mature C57BL/6 mice. *Osteoarthr Cartil*. 2022;30(12):1593-1605.
11. Li G, Yin J, Gao J, et al. Subchondral bone in osteoarthritis: insight into risk factors and microstructural changes. *Arthritis Res Ther*. 2013;15(6):223.
12. Madry H, van Dijk CN, Mueller-Gerbl M. The basic science of the subchondral bone. *Knee Surg Sports Traumatol Arthrosc*. 2010;18(4):419-433.
13. Botter SM, van Osch GJVM, Waarsing JH, et al. Cartilage damage pattern in relation to subchondral plate thickness in a collagenase-induced model of osteoarthritis. *Osteoarthr Cartil*. 2008;16(4):506-514.
14. Burr DB. Anatomy and physiology of the mineralized tissues: role in the pathogenesis of osteoarthrosis. *Osteoarthr Cartil*. 2004;12:20-30.
15. White MS, Brancati RJ, Lepley LK. Relationship between altered knee kinematics and subchondral bone remodeling in a clinically translational model of ACL injury. *J Orthop Res*. 2022;40(1):74-86.
16. Goldring SR. Role of bone in osteoarthritis pathogenesis. *Med Clin North Am*. 2009;93(1):25-35.
17. Lockwood KA, Chu BT, Anderson MJ, Haudenschild DR, Christiansen BA. Comparison of loading rate-dependent injury modes in a murine model of post-traumatic osteoarthritis. *J Orthop Res*. 2014;32(1):79-88.
18. Neogi T. Clinical significance of bone changes in osteoarthritis. *Ther Adv Musculoskelet Dis*. 2012;4(4):259-267.
19. Baht GS, Vi L, Alman BA. The role of the immune cells in fracture healing. *Curr Osteoporos Rep*. 2018;16(2):138-145.
20. Loeser RF, Collins JA, Diekman BO. Ageing and the pathogenesis of osteoarthritis. *Nat Rev Rheumatol*. 2016;12(7):412-420.
21. Barry F, Murphy M. Mesenchymal stem cells in joint disease and repair. *Nat Rev Rheumatol*. 2013;9(10):584-594.
22. Li G, Zheng Q, Landao-Bassonga E, et al. Influence of age and gender on microarchitecture and bone remodeling in subchondral bone of the osteoarthritic femoral head. *Bone*. 2015;77:91-97.
23. Chen H, Zhou X, Fujita H, Onozuka M, Kubo KY. Age-related changes in trabecular and cortical bone microstructure. *Int J Endocrinol*. 2013;2013:1-9.
24. Ferguson VL, Bushby AJ, Boyde A. Nanomechanical properties and mineral concentration in articular calcified cartilage and subchondral bone. *J Anat*. 2003;203(2):191-202.
25. Glatt V, Canalis E, Stadmeyer L, Bouxsein ML. Age-related changes in trabecular architecture differ in female and Male C57BL/6J mice. *J Bone Miner Res*. 2007;22(8):1197-1207.
26. Flurkey K, Currer J, Harrison D. *Mouse Models in Aging Research*. 2nd ed. Elsevier; 2007:637-672.
27. Anderson MJ, Diko S, Baehr LM, Baar K, Bodine SC, Christiansen BA. Contribution of mechanical unloading to trabecular bone loss following non-invasive knee injury in mice. *J Orthop Res*. 2016;34(10):1680-1687.
28. Ziemian SN, Witkowski AM, Wright TM, Otero M, van der Meulen MCH. Early inhibition of subchondral bone remodeling slows load-induced posttraumatic osteoarthritis development in mice. *J Bone Miner Res*. 2021;36(10):2027-2038.
29. Blaker CL, Clarke EC, Little CB. Using mouse models to investigate the pathophysiology, treatment, and prevention of post-traumatic osteoarthritis. *J Orthop Res*. 2017;35(3):424-439.
30. Onur TS, Wu R, Chu S, Chang W, Kim HT, Dang ABC. Joint instability and cartilage compression in a mouse model of posttraumatic osteoarthritis. *J Orthop Res*. 2014;32(2):318-323.
31. Hahn AK, Wallace CW, Welhaven HD, et al. The microbiome mediates epiphyseal bone loss and metabolomic changes after acute joint trauma in mice. *Osteoarthr Cartil*. 2021;29(6):882-893.

32. Ko FC, Dragomir C, Plumb DA, et al. In vivo cyclic compression causes cartilage degeneration and subchondral bone changes in mouse tibiae. *Arth Rheumat*. 2013;65(6):1569-1578.
33. Manitta L, Labrune M, Olive L, Fayolle C, Berteau JP. Subchondral bone alterations in a novel model of intermediate post traumatic osteoarthritis in mice. *J Biomech*. 2022;142:111233.
34. Hayami T, Pickarski M, Zhuo Y, Wesolowski GA, Rodan GA, Duong LT. Characterization of articular cartilage and subchondral bone changes in the rat anterior cruciate ligament transection and meniscectomized models of osteoarthritis. *Bone*. 2006;38(2):234-243.
35. Ramme AJ, Lendhey M, Raya JG, Kirsch T, Kennedy OD. A novel rat model for subchondral microdamage in acute knee injury: a potential mechanism in post-traumatic osteoarthritis. *Osteoarthr Cartil*. 2016;24(10):1776-1785.
36. Maerz T, Newton MD, Fleischer M, et al. Traumatic joint injury induces acute catabolic bone turnover concurrent with articular cartilage damage in a rat model of posttraumatic osteoarthritis. *J Orthop Res*. 2021;39(9):1965-1976.
37. Lin Y-Y, Christiansen BA. Non-invasive compression-induced anterior cruciate ligament (ACL) injury and in vivo imaging of protease activity in mice. *J Visualized Exp*. 2023;(199):e65249. doi:10.3791/65249
38. Chang JC, Sebastian A, Murugesh DK, et al. Global molecular changes in a tibial compression induced ACL rupture model of post-traumatic osteoarthritis. *J Orthop Res*. 2017;35(3):474-485.
39. Oliver WC, Pharr GM. An improved technique for determining hardness and elastic modulus using load and displacement sensing indentation experiments. *J Mater Res*. 1992;7(6):1564-1583.
40. Buie HR, Moore CP, Boyd SK. Postpubertal architectural developmental patterns differ between the L3 vertebra and proximal tibia in three inbred strains of mice. *J Bone Miner Res*. 2020;23(12):2048-2059.
41. Halloran BP, Ferguson VL, Simske SJ, Burghardt A, Venton LL, Majumdar S. Changes in bone structure and mass with advancing age in the male C57BL/6J mouse. *J Bone Miner Res*. 2002;17(6):1044-1050.
42. Cunningham HC, Orr S, Murugesh DK, et al. 2023. Differential bone adaptation to mechanical unloading and reloading in young, old, and osteocyte deficient mice. *Bone* 167:116646.

SUPPORTING INFORMATION

Additional supporting information can be found online in the Supporting Information section at the end of this article.

How to cite this article: Dauenhauer LA, Hislop BD, Brahmachary P, et al. Aging alters the subchondral bone response 7 days after noninvasive traumatic joint injury in C57BL/6JN mice. *J Orthop Res*. 2024;1-11. doi:10.1002/jor.25921